

Quantum impurity models coupled to Markovian and non-Markovian baths

Cite as: J. Chem. Phys. **151**, 044102 (2019); <https://doi.org/10.1063/1.5100157>

Submitted: 15 April 2019 . Accepted: 26 June 2019 . Published Online: 22 July 2019

Marco Schiro , and Orazio Scarlatella 

COLLECTIONS

Paper published as part of the special topic on [Dynamics of Open Quantum Systems](#)

Note: This paper is part of a JCP Special Topic on Dynamics of Open Quantum Systems.



View Online



Export Citation



CrossMark

ARTICLES YOU MAY BE INTERESTED IN

[Five approaches to exact open-system dynamics: Complete positivity, divisibility, and time-dependent observables](#)

The Journal of Chemical Physics **151**, 044101 (2019); <https://doi.org/10.1063/1.5094412>

[Non-Markovian stochastic Schrödinger equation in k-space toward the calculation of carrier dynamics in organic semiconductors](#)

The Journal of Chemical Physics **151**, 044115 (2019); <https://doi.org/10.1063/1.5096219>

[Open quantum dynamics of a three-dimensional rotor calculated using a rotationally invariant system-bath Hamiltonian: Linear and two-dimensional rotational spectra](#)

The Journal of Chemical Physics **151**, 044105 (2019); <https://doi.org/10.1063/1.5108609>

Lock-in Amplifiers
... and more, from DC to 600 MHz



Quantum impurity models coupled to Markovian and non-Markovian baths

Cite as: J. Chem. Phys. 151, 044102 (2019); doi: 10.1063/1.5100157

Submitted: 15 April 2019 • Accepted: 26 June 2019 •

Published Online: 22 July 2019



Marco Schiro^{1,a)}  and Orazio Scarlatella² 

AFFILIATIONS

¹JEIP, USR 3573 CNRS, Collège de France, PSL Research University, 11, place Marcelin Berthelot, 7 5231 Paris Cedex 05, France

²Institut de Physique Théorique, Université Paris Saclay, CNRS, CEA, F-91191 Gif-sur-Yvette, France

Note: This paper is part of a JCP Special Topic on Dynamics of Open Quantum Systems.

^{a)}On Leave from Institut de Physique Théorique, Université Paris Saclay, CNRS, CEA, F-91191 Gif-sur-Yvette, France.

Email: marco.schiro@ipht.fr.

ABSTRACT

We develop a method to study quantum impurity models, small interacting quantum systems bilinearly coupled to an environment, in the presence of an additional Markovian quantum bath, with a generic nonlinear coupling to the impurity. We aim at computing the evolution operator of the reduced density matrix of the impurity, obtained after tracing out all the environmental degrees of freedom. First, we derive an exact real-time hybridization expansion for this quantity, which generalizes the result obtained in the absence of the additional Markovian dissipation and which could be amenable to stochastic sampling through diagrammatic Monte Carlo. Then, we obtain a Dyson equation for this quantity and we evaluate its self-energy with a resummation technique known as the noncrossing approximation. We apply this novel approach to a simple fermionic impurity coupled to a zero temperature fermionic bath and in the presence of Markovian pump, losses, and dephasing.

Published under license by AIP Publishing. <https://doi.org/10.1063/1.5100157>

I. INTRODUCTION

Small interacting quantum systems coupled to external environments represent basic paradigms of transport, dissipation, and nonequilibrium phenomena. Understanding the dynamical behavior of these open quantum systems is therefore crucial in many different physical contexts where the idealization of an isolated quantum system obeying perfectly unitary quantum dynamics is either restrictive or unable to capture the fundamental physics.

In condensed matter physics, the motivation comes from studying models of quantum dissipation and macroscopic quantum tunneling in the early days of Caldeira-Leggett and spin-boson models^{1,2} which keep attracting a lot of interest³ or from diluted magnetic impurities in metals⁴ and transport through quantum dots and single molecules attached to leads,^{5–8} leading to fermionic realizations of so-called quantum impurity models. These consist of small quantum systems with few interacting degrees of freedom, the impurity, coupled via hybridization to a gapless reservoir of fermionic or

bosonic excitations. The dynamical correlations of such reservoirs, which decay in time as a power law at zero temperature and feature strong memory effects,⁹ together with a local many body interaction, make quantum impurity physics highly nontrivial. Nevertheless, methods to solve the dynamics of quantum impurity models have flourished in recent years, mainly driven by the developments of diagrammatic Monte Carlo.^{10–18}

On a different front, recent advances in quantum optics, quantum electronics, and quantum information science have brought forth novel classes of driven open quantum systems in which excitations are characterized by finite lifetime due to unavoidable losses, dephasing, and decoherence processes originating from their coupling to an external electromagnetic environment. Examples include atomic and optical systems such as ultracold gases in optical lattices¹⁹ or trapped ions,²⁰ as well as solid state systems such as arrays of nonlinear superconducting microwave cavities.^{21,22} In these settings, the dissipative processes associated with the external environment can be very well described in terms of a Lindblad master equation for the system density matrix.²³ A major effort here is to

conceive situations in which coupling to a quantum environment can involve nonlinear combinations of system operators, thus mediating effective interactions which act as a resource for quantum state preparation and to engineer a desired steady state. Such a dissipation engineering is actively investigated in quantum optics.^{24–26} This has stimulated a new wave of interest around open Markovian quantum systems at the interface between quantum optics and condensed matter physics.

The examples above represent two well studied, yet substantially separated, paradigms of open quantum systems. At the same time, much less is known about the interface between those two settings, namely, the interplay between Markovian dissipation and the coupling to a fully structured, frequency dependent, non-Markovian quantum bath, especially for what concerns the emergent many body physics. Interest around these new kind of quantum impurity problems has recently grown.^{27–29} Such a question is potentially relevant in a number of contexts. From one side, mesoscopic quantum devices have been successfully coupled to electromagnetic resonators hosting dissipative photon fields,^{30–33} offering the possibility to investigate the fate of exotic many body phases such as the Kondo effect in the presence of Markovian dissipation.

On the other hand, in the context of quantum optics and quantum information, the role of non-Markovian bath correlations has been recently attracting enormous interest^{34–36} and there is an urgent need to develop novel theoretical approaches to address this question.

With these motivations, in this work, we focus on a model for a quantum impurity coupled to two kinds of external environments, as depicted in Fig. 1: a quantum bath described by a set of noninteracting modes bilinearly coupled to our impurity degree of freedom, as in conventional quantum impurity models, resulting in a frequency dependent non-Markovian evolution for the impurity and a second environment, where the noninteracting bath modes can also be nonlinearly coupled to the impurity, but for which the reduced impurity dynamics would be well described by a Markovian master equation. The resulting impurity problem encodes therefore the interplay between those two kinds of dissipative mechanisms and the local interaction on the impurity.

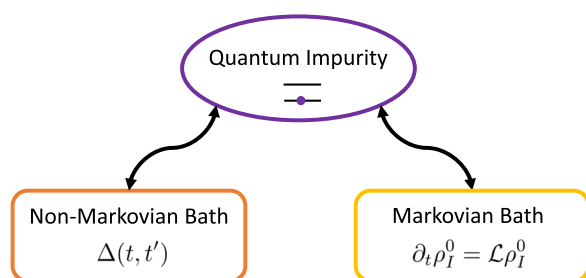


FIG. 1. Schematic plot of the setup considered in this manuscript. A small quantum system (impurity) is (i) bilinearly coupled to a quantum bath whose nontrivial correlations, encoded in the hybridization function $\Delta(t, t')$, lead to non-Markovian behavior and (ii) coupled nonlinearly to a Markovian bath whose effect on the impurity is described by a Lindblad master equation. The resulting quantum impurity model with mixed Markovian and non-Markovian dissipation is studied using hybridization expansion techniques.

Taking inspiration from recent developments in quantum impurity physics,^{10,11,13,37} we develop here a hybridization expansion for the real-time evolution operator of the impurity, obtained after tracing out both the non-Markovian environment, as usually done in the literature, and the Markovian bath. The final result naturally generalizes the well known real-time hybridization expansions to this mixed Markovian/non-Markovian context. In addition to its own interest and potential for the development of diagrammatic Monte Carlo sampling, this expansion allows us to formulate a self-consistent resummation technique for the real-time impurity evolution operator based on the noncrossing approximation (NCA) used in the context of quantum impurity models.^{38–43} We derive and discuss in detail this approach and test it on a simple fermionic model coupled to a zero temperature bath and in the presence of Markovian dissipation.

The paper is organized as follows. In Sec. II, we introduce the model and the general formulation of the problem. Section III is devoted to derive the hybridization expansion for the real-time impurity propagator, after tracing out the non-Markovian bath (Sec. III A) and the Markovian environment (Sec. III B). In Sec. IV, we develop a self-consistent resummation based on the noncrossing approximation, while in Sec. V we apply this method to a simple model.

II. MODEL AND GENERAL FORMULATION OF THE PROBLEM

We consider a model of a quantum impurity, a small quantum system with a finite number of bosonic/fermionic degrees of freedom $[d_a, d_b]_{\pm} = \delta_{ab}$ and with Hamiltonian $H_I[d_a, d_a^{\dagger}]$, coupled to two different quantum baths (see Fig. 1). We will denote the Hamiltonian of the baths with H_M and $H_{\bar{M}}$, where the subscripts refer to the fact that \bar{M} is a non-Markovian bath and M is a Markovian one. We describe the two environments as a collection of noninteracting bosonic/fermionic modes (respectively, if the impurity is bosonic/fermionic)

$$H_M = \sum_p \omega_p b_p^{\dagger} b_p \quad H_{\bar{M}} = \sum_k \epsilon_k c_k^{\dagger} c_k. \quad (1)$$

The total Hamiltonian therefore reads

$$H = H_I + H_M + H_{IM} + H_{\bar{M}} + H_{I\bar{M}},$$

where we have introduced the two coupling terms between the impurity and the M and \bar{M} baths. We will consider the impurity to be bilinearly coupled to the \bar{M} bath, i.e., through a coupling Hamiltonian of the form

$$H_{I\bar{M}} = \sum_{ka} V_{ka} (d_a^{\dagger} c_k + \text{h.c.}), \quad (2)$$

while the coupling between the impurity and the M bath is taken of the most general form for which one can derive a Lindblad master equation,⁴⁴

$$H_{IM} = \sum_{\alpha} X_{\alpha} B_{\alpha} \quad (3)$$

with $X_{\alpha} = X_{\alpha}^{\dagger}$ and $B_{\alpha} = B_{\alpha}^{\dagger}$ generic operators, respectively, of the impurity and of the Markovian bath.

Defining the time evolution operator of the entire system as $U(t, 0) = e^{-iHt}$ and given an initial condition for the system density matrix $\rho(0)$, we can formally write down the reduced density matrix of the impurity at time t , tracing out the degrees of freedom of the two environments

$$\rho_I(t) = \text{tr}_{M\bar{M}}[U(t, 0)\rho(0)U^\dagger(t, 0)] \quad (4)$$

from which the dynamics of simple impurity observables can be readily obtained as $O_I(t) = \text{tr}[\rho_I(t)O_I]$. With the assumption that the initial density operator of the environment and the impurity factorizes,⁴⁴ we can define the evolution operator of the reduced dynamics

$$\rho_I(t) = \mathcal{V}(t, 0)\rho_I(0). \quad (5)$$

This reduced density operator and its evolution operator are the key quantities over which we will focus our attention throughout the manuscript. Performing the trace over the environment degrees of freedom is a highly nontrivial problem. In the following, we will obtain two main results. The first one is a formal series from \mathcal{V} to all orders in the coupling with the non-Markovian bath, called hybridization expansion, and the second one is a closed equation for \mathcal{V} , based on a self-consistent resummation of the series.

We stress that the order in which the trace over the two environments is taken in Eq. (4) is not crucial. While in this paper we will proceed by first taking the trace over the non-Markovian environment, resulting in a hybridization expansion, and then over the Markovian one, we could have equally reversed this choice and still obtain the same final result.

III. HYBRIDIZATION EXPANSION

In this section, we derive a formal hybridization expansion (21) for the reduced density matrix of the impurity. Such an expansion is usually derived in the context of quantum impurity models coupled to a single bath, as a starting point to develop exact Monte-Carlo sampling^{11,37} or approximated resummation techniques^{41,45} to solve the problem. There, the formulation is typically done at the level of the partition function, i.e., tracing out also the impurity degrees of freedom, while we are interested in the reduced density matrix and the evolution operator, see Eq. (5); therefore, we will not perform such a trace, a fact that will result in some formal difference in the approach. More importantly, here the quantum impurity is also coupled to a second Markovian environment that we will need to trace out as well and this can be done exactly under the assumption that the IM subsystem obeys a Markovian Lindblad master equation.^{44,46}

A. Tracing over the non-Markovian bath

We begin by performing the trace over the non-Markovian environment which is quadratic in terms of bath operators and bilinearly coupled to the impurity. Such a trace could be performed exactly within a path integral formulation leading to an effective Keldysh action which is nonlocal in time. Here, we proceed instead at the operator level by noticing that the trace could be taken exactly order by order in an expansion in the coupling between the non-Markovian environment and the impurity.

In order to derive this expansion, we write down the full Hamiltonian of the system as $H = H_0 + H_{\bar{M}} + H_{IM}$, describing, respectively, the impurity embedded in the Markovian bath ($H_0 = H_I + H_M + H_{IM}$), the non-Markovian environment, and its coupling to the impurity. We then move to the interaction picture with respect to the Hamiltonian $H_0 + H_{\bar{M}}$. Introducing the standard time-ordering and anti-time-ordering operators T_I and \check{T}_I , the density operator becomes

$$\rho(t) = e^{-i(H_0+H_{\bar{M}})t} T_I e^{-i \int_0^t dt' H_{IM}(t')} \rho(0) \check{T}_I e^{i \int_0^t dt' H_{IM}(t')} e^{i(H_0+H_{\bar{M}})t}. \quad (6)$$

We will perform a simultaneous expansion in powers of $H_{IM}(t')$ both on the left and on the right of the initial density operator $\rho(0)$. A formal way to manage a single series expansion and to write all the operators on the left side of the density operator is to use the formalism of the Schwinger/Keldysh double contour $C(t, 0)$ ^{47,48} (Fig. 2). Operators on the left (right) side of $\rho(0)$ are assigned a + or - label so that the couple $(t, \gamma) \equiv t_\gamma$ with $\gamma \in \{+, -\}$ allows us to locate one operator on this double time-axis.

We introduce the standard Keldysh time-ordering on the contour as follows:

$$t_\gamma > t_{\gamma'} \quad \text{if} \quad \begin{cases} t > t', & \gamma = \gamma' = + \\ t < t', & \gamma = \gamma' = - \\ \gamma = -, & \gamma' = + \end{cases} \quad (7)$$

This ordering allows us to define a time-ordering operator T_C such that two operators X_1 and X_2 , with X being a creation or annihilation fermionic (bosonic) operator, anticommute (commute) under time-ordering: $T_C X_1(t_\gamma) X_2(t_{\gamma'}) = \xi T_C X_2(t_{\gamma'}) X_1(t_\gamma)$, with

$$\begin{aligned} \xi &= 1 & \text{for bosons,} \\ \xi &= -1 & \text{for fermions.} \end{aligned}$$

The time ordering operator is defined as follows:

$$T_C X_1(t_\gamma) X_2(t_{\gamma'}) = \begin{cases} X_1(t_\gamma) X_2(t_{\gamma'}) & \text{for } t_\gamma > t_{\gamma'} \\ \xi X_2(t_{\gamma'}) X_1(t_\gamma) & \text{for } t_\gamma < t_{\gamma'} \end{cases}, \quad (8)$$

which naturally extends to the case of n operators. Once time ordered, the operators belonging to the - branch of the contour has to be brought on the right side of the density matrix, as if there we were exploiting the cyclic property of a trace.

By defining contour integrals as $\int_{C(0,t)} dt \equiv \int_0^t dt_+ - \int_0^t dt_-$, one can show that the density operator evolution (6) can be written in the compact form,

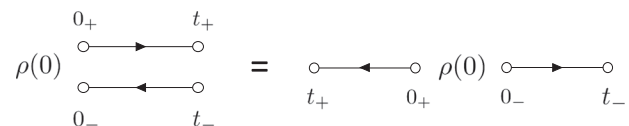


FIG. 2. Two equivalent pictorial representations of the Schwinger/Keldysh contour $C(t, 0)$, describing the nonequilibrium evolution of an initial density operator $\rho(0)$ from time 0 to time t . The two branches of the contour are usually called + and -, and they correspond to the two time evolution operators applied to the left and to the right of the initial density operator, as in Eq. (6).

$$\rho(t) = T_C e^{-i(H_0+H_M)(t_+-t_-)} e^{-i \int_{C(0,t)} dt' H_{IM}(t')} \rho(0)$$

and, accordingly, the evolution operator defined in (5) can be written as

$$\mathcal{V}(t,0)\rho_I(0) = \text{tr}_{MM} \left[T_C e^{-iH_0(t_+-t_-)} e^{-i \int_{C(0,t)} dt' H_{IM}(t')} \rho(0) \right]. \quad (9)$$

In order to perform the partial trace on the non-Markovian environment, we assume that at time $t = 0$ there is no entanglement between the non-Markovian bath and the rest of the system such that the density operator factorizes $\rho(0) = \rho_{IM}(0) \otimes \rho_M(0)$, with $\rho_M(0)$ quadratic in bosonic/fermionic operators. Initial thermal states could be taken into account considering a third, imaginary time branch of the

nonequilibrium contour,^{49–51} but this is beyond the interest of this work.

We then Taylor-expand the time-ordered exponential in power of the impurity-bath hybridization H_{IM} and perform the trace over the bath degrees of freedom, which immediately reduces the expansion to only even order terms. Then, using Wick's theorem and performing the sums over $\{b_i, b'_i\}$, we can write the final result in terms of the bath hybridization function,

$$\Delta_{a'a}^{y'y}(t',t) \equiv \sum_{b'} V_{a'b'} V_{ab'}^* G_{b'}(t'_y, t_y), \quad (10)$$

where $G_{b'}(t'_y, t_y) = -i \langle T_C c_{b'}(t'_y) c_{b'}^\dagger(t_y) \rangle$ is the contour ordered bath Green's function. Finally, we obtain the hybridization expansion,^{45,52}

$$\begin{aligned} \mathcal{V}(t,0)\rho_I(0) &= \sum_{k=0} \frac{(-i)^k}{k!^2} \sum_{\gamma_1 \dots \gamma'_k} \prod_i \gamma_i \gamma'_i \sum_{a_1 \dots a'_k} \int_0^t dt_1 \dots \int_0^t dt'_k \text{tr}_M \left[T_C e^{-iH_0(t_+-t_-)} d_{a'_k}^\dagger(t'_k, \gamma'_k) d_{a_k}(t_k, \gamma_k) \dots d_{a_1}(t_1, \gamma_1) \rho_{IM}(0) \right] \\ &\times \sum_{\sigma \in P} \xi^{\text{sign}(\sigma)} \Delta_{a'_1 a_{\sigma(1)}}^{y'_1 y_{\sigma(1)}}(t'_1, t_{\sigma(1)}) \dots \Delta_{a'_k a_{\sigma(k)}}^{y'_k y_{\sigma(k)}}(t'_k, t_{\sigma(k)}). \end{aligned} \quad (11)$$

γ_i, γ'_i are contour indices $\gamma \in \{+, -\}$. We notice that the hybridization function $\Delta_{a'_i a_{\sigma(i)}}^{y'_i y_{\sigma(i)}}(t'_i, t_{\sigma(i)})$ connects the $d_{a_{\sigma(i)}}(t_{\sigma(i)}, \gamma_{\sigma(i)})$ operator with the $d_{a'_i}^\dagger(t'_i, \gamma'_i)$ one. We can interpret this construction as follows. The d operator creates a “hole” in the impurity, which is propagated through the system and then annihilated by a d operator. To this hole, it corresponds (from the definition of Δ) a particle of the environment which is created, propagated, and annihilated. Thus, the series eventually describes processes in which particles hop from the impurity to the environment and back to the impurity.

B. Tracing over the Markovian bath

1. Superoperator formalism

It is useful to describe time-evolution using superoperators, as these are natural objects to describe the dynamics of open systems and since they provide a useful framework to work out the trace on the Markovian environment in Eq. (11). We call the superoperator an operator that acts on an operator, rather than on a quantum state. The focus is shifted from the standard evolution operator $U(t,0) = e^{-iHt}$, which evolves a pure state (a ket) in time, to the superoperator $\mathcal{U}(t,0)$ which time-evolves a density operator and is defined by

$$\rho(t) = U(t,0)\rho(0)U(0,t) \equiv \mathcal{U}(t,0)\rho(0). \quad (12)$$

We can write a generic time-ordered string of operators, like it appears in Eq. (11), in Schrödinger's picture and in a compact form, using the superoperator notation. This comes at the price of introducing some notation.

We promote d, d^\dagger operators in Schrödinger's picture to superoperators $d_\gamma, d_\gamma^\dagger$, with a contour index γ reminiscent of the branch

the original operators belonged to,

$$d_\gamma^\dagger[\bullet] = \begin{cases} d^\dagger \bullet & \text{if } \gamma = + \\ \bullet d^\dagger & \text{if } \gamma = - \end{cases}. \quad (13)$$

We trivially generalize the contour time-ordering operator T_C to the superoperator notation

$$\begin{aligned} T_C X_{1(t,\gamma)} \mathcal{U}_0(t,t') X_{2(t',\gamma')} \\ = \begin{cases} X_{1(t,\gamma)} \mathcal{U}_0(t,t') X_{2(t',\gamma')} & \text{for } (t,\gamma) > (t',\gamma') \\ \xi X_{2(t',\gamma')} \mathcal{U}_0(t',t) X_{1(t,\gamma)} & \text{for } (t,\gamma) < (t',\gamma') \end{cases}. \end{aligned} \quad (14)$$

The $X_{t,\gamma}$ superoperators are objects in Schrödinger's picture, and their time label t is just meant to know how to order them.

We also need to introduce a further “forward” time-ordering operator T_F , which orders two superoperators according to their time labels t, t' , regardless of their contour index,

$$\begin{aligned} T_F X_{1(t,\gamma)} \mathcal{U}_0(t,t') X_{2(t',\gamma')} \\ = \begin{cases} X_{1(t,\gamma)} \mathcal{U}_0(t,t') X_{2(t',\gamma')} & \text{for } t > t' \\ X_{2(t',\gamma')} \mathcal{U}_0(t',t) X_{1(t,\gamma)} & \text{for } t < t' \end{cases}. \end{aligned} \quad (15)$$

This definition is the same for both fermions and bosons, with no extra minus signs for fermions.

Using these definitions, we can write the following identity:

$$\begin{aligned} T_C e^{-iH_0(t_+-t_-)} d^\dagger(t'_k) \dots d(t_1) \rho_{IM}(0) \\ = T_F T_C \mathcal{U}_0(t, t'_k) d_{t'_k \gamma'_k}^\dagger \mathcal{U}_0(t'_k, t_{k-1}) \dots d_{t_1 \gamma_1} \mathcal{U}_0(t_1, 0) \rho_{IM}(0). \end{aligned} \quad (16)$$

The second line is a chain of subsequent time-evolutions operated by \mathcal{U}_0 , going overall from time 0 to time t , alternated with the application of $d_\gamma, d_\gamma^\dagger$ superoperators. We remark that the two time-order operators T_C and T_F do not commute. In order to evaluate the second line of Eq. (16), one has first to order the superoperators

according to T_C ; this first ordering is necessary in order to compute the nontrivial sign factor obtained by swapping fermionic operators. Then, the superoperators must be reordered according to the “forward” time-ordering operator T_F . This insures that, in order to evaluate Eq. (16), one has to apply only forward in time evolution superoperators.

2. Performing the partial trace

We now aim at performing the partial trace on the Markovian environment which is left in Eq. (11). This trace is taken on a contour time-ordered string of impurity operators. The latter are nevertheless evolved by the joint dynamics of the impurity plus the remaining bath, making the partial trace nontrivial to evaluate. Assuming that the impurity-bath dynamics is governed by a Lindblad master equation, then the partial trace becomes trivial.^{46,53} We report a proof here as this is a crucial step to obtain the hybridization expansion (21). We recall the Lindblad master equation,^{44,46}

$$\partial_t \rho_I^0 = -i[H_I, \rho_I^0] + \sum_{\alpha} \gamma_{\alpha} \left(L_{\alpha} \rho_I^0 L_{\alpha}^{\dagger} - \frac{1}{2} \{ L_{\alpha}^{\dagger} L_{\alpha}, \rho_I^0 \} \right), \quad (17)$$

where L_{α} are the jump operators, microscopically determined by the environment-impurity coupling (3). $\rho_I^0(t)$ must not be confused with $\rho_I(t) = \text{tr}_M \rho_{IM}(t)$, as the former is the density operator obtained by evolving $\rho(0)$ in the presence of the Markovian environment alone. $\rho_I(t)$ instead is obtained by evolving $\rho(0)$ with a dynamics that includes both the Markovian and non-Markovian environments. Defining the Markovian evolution superoperator,

$$\mathcal{V}_0(t - t') = e^{\mathcal{L}(t-t')}, \text{ with } t > t', \text{ then}$$

$$\rho_I^0(t) = \mathcal{V}_0(t - t') \rho_I(0). \quad (18)$$

We remark that \mathcal{V}_0 depends only on time differences as it satisfies (17). This is equivalent to

$$\text{tr}_M \rho_{IM}^0(t) = \text{tr}_M [\mathcal{U}_0(t, t') \rho_{IM}^0(t')] = \mathcal{V}_0(t - t') \text{tr}_M \rho_{IM}^0(t'). \quad (19)$$

In order to show how to perform the trace of the string of superoperators in (16), let us assume that time ordering is already enforced so that we do not have to care about it. Defining $r_1(t) = \mathcal{U}_0(t, t'_k) r_1(t'_k)$ and $r_1(t'_k) = d_{t'_k, \gamma'_k}^{\dagger} \mathcal{U}_0(t'_k, t_{k-1}) \dots d_{t_1, \gamma_1} \mathcal{U}_0(t_1, 0) \rho_{IM}(0)$, we can break down the tracing operation as follows:

$$\begin{aligned} \text{tr}_M [\mathcal{U}_0(t, t'_k) d_{t'_k, \gamma'_k}^{\dagger} \dots d_{t_1, \gamma_1} \mathcal{U}_0(t_1, 0) \rho_{IM}(0)] \\ = \text{tr}_M r_1(t) = \text{tr}_M [\mathcal{U}_0(t, t'_k) r_1(t'_k)] = \mathcal{V}_0(t - t') \text{tr}_M r_1(t'_k). \end{aligned} \quad (20)$$

The last equality is analogous to Eq. (19) and holds under the same assumptions leading to the Lindblad master equation. One can iterate this procedure, as now $\text{tr}_M r_1(t'_k) = d_{t'_k, \gamma'_k}^{\dagger} \text{tr}_M [\mathcal{U}_0(t'_k, t_{k-1}) r_2(t_{k-1})]$, to turn all the \mathcal{U}_0 superoperators in Eq. (11) into \mathcal{V}_0 ones.

3. Generalized hybridization expansion

We then get to the final form of the hybridization expansion in the presence of both a non-Markovian and a Markovian environment, which is one of the main results of this work,

$$\begin{aligned} \mathcal{V}(t, 0) = \sum_{k=0} \frac{(-i)^k}{k!^2} \sum_{\gamma_1 \dots \gamma'_k} \prod_i \gamma_i \gamma'_i \sum_{a_1 \dots a'_k} \int_0^t dt_1 \dots \int_0^t dt'_k T_{FC} \mathcal{V}_0(t, t'_k) d_{a'_k, \gamma'_k}^{\dagger} \mathcal{V}_0(t'_k, t_{k-1}) \dots d_{a_1, \gamma_1} \mathcal{V}_0(t_1, 0) \\ \times \sum_{\sigma \in P} \xi^{\text{sign}(\sigma)} \Delta_{a'_1, a_{\sigma(1)}}^{\gamma'_1, \gamma_{\sigma(1)}}(t'_1, t_{\sigma(1)}) \dots \Delta_{a'_k, a_{\sigma(k)}}^{\gamma'_k, \gamma_{\sigma(k)}}(t'_k, t_{\sigma(k)}). \end{aligned} \quad (21)$$

This series can be sampled using stochastic sampling techniques^{11,37,54} or approximately resummed.^{41,45} For both purposes, it is useful to define the Feynman rules for the series (21).

4. Matrix representation

Each term of the hybridization expansion (21) must be understood as a composition of applications of superoperators, from the right-most to the left-most one, on the initial density operator. We remark that in the usual representation in which states of the Hilbert space are vectors and operators are matrices, superoperators are rank-4 tensors. Instead, if we write operators as vectors, then superoperators become matrices. This is convenient to evaluate terms of the hybridization expansion (21) as matrix products. Namely,

$$\begin{aligned} \mathcal{V}_0(t, t'_k) d_{a'_k, \gamma'_k}^{\dagger} \dots d_{a_1, \gamma_1} \mathcal{V}_0(t_1, 0) \rho_I(0) \\ \rightarrow \bar{\mathcal{V}}_0(t, t'_k) \bar{d}_{a'_k, \gamma'_k}^{\dagger} \dots \bar{d}_{a_1, \gamma_1} \bar{\mathcal{V}}_0(t_1, 0) |\rho_I(0)\rangle \end{aligned} \quad (22)$$

using double bars to indicate matrices. Operators are represented as vectors in a space which is the tensor product (indicated with \otimes) of two copies of the original Hilbert space. The vectorization procedure, taking the example of the density operator, reads

$$\rho = \sum_{n,m} \rho_{nm} |n\rangle \langle m| \rightarrow \sum_{n,m} \rho_{nm} |n\rangle \otimes |m\rangle \equiv |\rho\rangle. \quad (23)$$

The matrices $\bar{\mathcal{V}}, \bar{d}_{\pm}, \bar{d}_{\pm}^{\dagger}$ corresponding to the superoperators $\mathcal{V}, d_{\pm}, d_{\pm}^{\dagger}$ are defined by the following simple procedure. Let us consider the superoperator $\mathcal{S} \bullet = A \bullet B$. Representing ρ as a vector $|\rho\rangle$, then also $\mathcal{S}\rho$ will be represented as a vector according to Eq. (23). It is simple to show that $|\mathcal{S}\rho\rangle = \bar{\mathcal{S}}|\rho\rangle$ defining $\bar{\mathcal{S}} = \bar{A} \otimes \bar{B}^T$. The matrix form of $d_{\pm}, d_{\pm}^{\dagger}$ in the doubled Hilbert space is

$$\begin{aligned} \bar{d}_{+} &= \bar{d} \otimes \bar{\mathbb{1}}, & \bar{d}_{+}^{\dagger} &= \bar{d}^{\dagger} \otimes \bar{\mathbb{1}}, \\ \bar{d}_{-} &= \bar{\mathbb{1}} \otimes \bar{d}^T, & \bar{d}_{-}^{\dagger} &= \bar{\mathbb{1}} \otimes \bar{d}^*. \end{aligned}$$

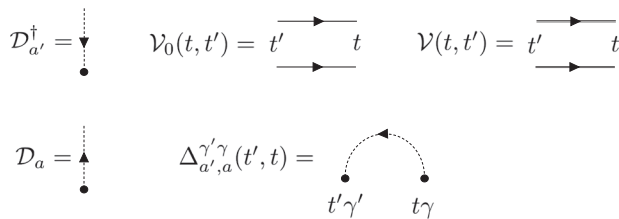


FIG. 3. The Feynman rules to represent the hybridization expansion (21). The arrow of the hybridization line Δ goes from a d superoperator to the first d^\dagger one.

with \bar{d}_\pm^\dagger as the hermitian conjugate of \bar{d}_\pm . These rules allow us to obtain the matrix representation of the Liouvillian and then of \mathcal{V}_0 .

C. Feynman rules

The Feynman rules to draw the hybridization expansion (21) are represented in Fig. 3. We will use these rules to draw a term with $2k$ annihilation and creation superoperators, with a particular ordering for the times $\{t_i, t'_i \dots t_1, t'_1\}$ and a choice of a permutation $\{\sigma(1), \sigma(2), \dots, \sigma(k)\}$. To do that, we draw a couple of parallel axes representing the double contour from time $t = 0$ to time t . d_γ (d_γ^\dagger) superoperators are represented as a dashed half-line with outwards (inwards) arrows, stemming from the contour branch γ . The dashed half-lines corresponding to the superoperators $d_{a'_i}^\dagger(t'_i, \gamma'_i)$ and $d_{a_{\sigma(i)}}(t_{\sigma(i)}, \gamma_{\sigma(i)})$ are joined together to form a hybridization line, representing the hybridization function $\Delta_{a'_i a_{\sigma(i)}}^{\gamma'_i \gamma_{\sigma(i)}}(t'_i, t_{\sigma(i)})$, which has an arrow going from d to d^\dagger . Then, each part of the double contour between two integration times, drawn as two parallel solid segments, represents a time-propagation superoperator \mathcal{V}_0 . The dressed evolution operator \mathcal{V} is drawn by replacing the contour solid lines by double lines. As an example, the diagram corresponding to

$$i \int_0^t dt_1 \int_0^{t_1} dt'_1 \mathcal{V}_0(t, t'_1) d_{a'_1}^\dagger \mathcal{V}_0(t'_1, t_1) d_{a_1} \mathcal{V}_0(t_1, 0) \Delta_{a'_1 a_1}^{\gamma'_1 \gamma_1}(t'_1, t_1) \quad (24)$$

is shown in Fig. 4. All the diagrams with $2k$ annihilation and creation superoperators are generated by connecting d^\dagger superoperators to d

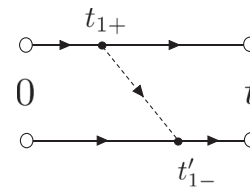


FIG. 4. The Feynman diagram representing Eq. (24).

ones in all possible choices of permutations σ and considering all possible time orderings of integration times.

IV. SELF-CONSISTENT DIAGRAMMATIC RESUMMATION TECHNIQUES

In this section, we start from the hybridization expansion derived in Sec. III, which involves bare diagrams to all orders, and use the Feynman rules to introduce diagrammatic resummation techniques.

To proceed further, it is useful to draw more compact diagrams where the double contour is collapsed on a single time-axis and thus a time propagation \mathcal{V}_0 is represented by a single line, as we show in Fig. 5. These compact diagrams represent an ensemble of diagrams drawn with the rules we introduced in Fig. 3.

The advantage of this notation is that all the diagrams represented by a single compact diagram have the same topology in terms of being 1-particle irreducible or noncrossing. Figure 6 shows the hybridization expansion drawn using these compact diagrams.

A. Dyson equation

As a first step, it is useful to distinguish diagrams which are one-particle irreducibles, i.e., compact diagrams which cannot be separated, by cutting a solid line, in two parts that are not connected by any hybridization line, as indicated in Fig. 6. Then, we introduce the self-energy Σ as the sum of one particle irreducible (1PI) diagrams. All the non-1PI diagrams can be obtained by joining some 1PI diagrams with solid lines; thus, the whole series can be written as

$$\mathcal{V} = \mathcal{V}_0 + \mathcal{V}_0 \circ \Sigma \circ \mathcal{V}_0 + \mathcal{V}_0 \circ \Sigma \circ \mathcal{V}_0 \circ \Sigma \circ \mathcal{V}_0 + \dots$$

We remark that the objects composing this series, \mathcal{V}_0 and Σ , are superoperators and the series must be understood as a composition of applications of superoperators, from the right-most to the

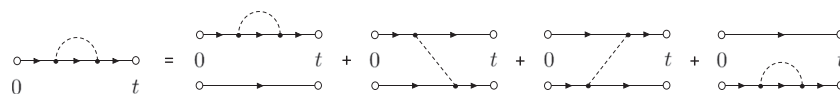


FIG. 5. Compact diagrams represent an ensemble of diagrams hiding the double contour structure. By omitting the arrows on hybridization lines, we mean that all the possible choices must be considered.

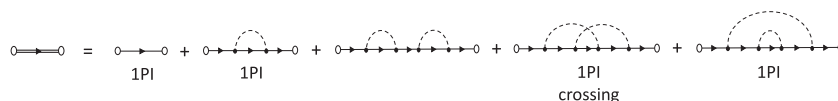


FIG. 6. 1PI diagrams of the hybridization expansion in Eq. (21).

left-most one, on a target operator. Self-energies and propagators are joined by the circle operation, \circ , standing for a superoperator application and a partial time convolution. Using brackets to stress that we refer to a superoperator application and the symbol \bullet to indicate a target operator, we have

$$\Sigma(t, t_1) \circ \mathcal{V}_0(t_1, t') \equiv \int_{t'}^t dt_1 \Sigma(t, t_1) [\mathcal{V}_0(t_1, t') [\bullet]].$$

The series above sums up to the Dyson equation $\mathcal{V} = \mathcal{V}_0 + \mathcal{V}_0 \circ \Sigma \circ \mathcal{V} = \mathcal{V}_0 + \mathcal{V} \circ \Sigma \circ \mathcal{V}_0$, or equivalently, in the integro-differential form

$$\partial_t \mathcal{V}(t, t') = \mathcal{L} \mathcal{V}(t, t') + \int_{t'}^t dt_1 \Sigma(t, t_1) \mathcal{V}(t_1, t'). \quad (25)$$

When the self-energy of the non-Markovian environment Σ is set to zero, this equation yields $\mathcal{V}(t) = e^{\mathcal{L}t}$, which is the Lindblad evolution.

One of the main effects of dissipative dynamics is that the system may forget about initial conditions and reach the same stationary state for any initial condition. Assuming a stationary state exists for a non-Markovian map \mathcal{V} defined by the Dyson equation (25), then it satisfies

$$\left(\mathcal{L} + \int_0^\infty dt_1 \Sigma(\infty, t_1) \right) \rho_{ss} = 0. \quad (26)$$

Setting the non-Markovian self-energy to zero, this equation reduces to the Lindblad condition for the stationary state. The derivation of this equation is in the [supplementary material](#).

B. The noncrossing approximation

The noncrossing approximation (NCA) corresponds to approximating the series for \mathcal{V} , and thus also for Σ , by considering only the compact diagrams in which the hybridization lines do not cross.^{38–41} The NCA diagrams composing the self-energy are shown in [Fig. 7](#).

In order to prove the second equality in [Fig. 7](#), we remark that the first and last times of a self-energy diagram must be connected together by a hybridization line. If it is not the case, in fact, the resulting diagram is either non-1PI or crossed. Then, all the diagrams of Σ (in NCA) are obtained connecting the intermediate times to form all the possible noncrossing diagrams (not only the 1PI ones this time). But the latter diagrams in turn define the NCA series for \mathcal{V} . This proves the second equality in [Fig. 7](#). We remark that then, the NCA self-energy coincides with its contributions (with $k = 1$), where the bare propagator \mathcal{V}_0 is replaced with the dressed one \mathcal{V} .

To obtain an analytic expression of the self-energy, we have to cast the $k = 1$ term of the hybridization expansion (21) in a form in which the innermost integration time is lower than the outermost, that is, with integrals of the form $\int_{t'}^t dt_1 \int_{t_1}^{t_1} dt_2$. In doing so, one must deal with the signs coming out of the time ordering. We report the calculation in the [supplementary material](#).

The expression for the self-energy eventually reads

$$\begin{aligned} \Sigma(t_1, t_2) = & \sum_{a,b} \sum_{\alpha\beta \in \{+,-\}} -\alpha^{(1+\xi)/2} \beta i \left[\Delta_{ba}^{\beta\alpha}(t_1, t_2) d_{\beta b}^\dagger \mathcal{V}(t_1, t_2) d_{aa} \right. \\ & \left. + \xi \Delta_{ab}^{\alpha\beta}(t_2, t_1) d_{\beta b} \mathcal{V}(t_1, t_2) d_{aa}^\dagger \right], \end{aligned} \quad (27)$$

where $\alpha, \beta \in \{+, -\}$ are contour indices and a, b are the fermionic generic indices.

We can interpret the two terms in [Eq. \(27\)](#) as follows. The first term propagates a hole in the impurity (applies d^\dagger first and then d) and a particle in the bath, the latter being described by a hybridization function with the same time arguments of \mathcal{V} . The second term propagates a particle in the impurity and a hole in the bath with a hybridization function with opposite time arguments than \mathcal{V} .

Few comments are in order here, concerning the above result. First, in the absence of the Markovian environment, that is, by replacing $\mathcal{V}(t, t')$ and $\mathcal{V}_0(t, t')$ with $\mathcal{U}(t, t')$ and $\mathcal{U}_0(t, t')$, our results are equivalent to nonequilibrium NCA schemes for unitary dynamics.^{40,42,43} There is a formal difference consisting in our superoperator formulation of the hybridization expansion and of the Dyson equation that is necessary to consider the additional Markovian environment without further approximations, but this difference is only formal and does not affect the results. In fact, if N is the dimensionality of the impurity Hilbert space, the usual nonequilibrium NCA propagator^{42,43} has different Keldysh components, each of them being an $N \times N$ matrix, while our \mathcal{V} propagator is a $N^2 \times N^2$ matrix with no Keldysh components.

Furthermore, the result obtained for the NCA self-energy in [Eq. \(27\)](#) makes clear that for a bath hybridization which is delta-correlated in time the resulting self-energy contribution to the Dyson equation takes the form of an additional Lindblad dissipator. In other words, one can recover the Lindblad master equation from our diagrammatic NCA approach in the Markovian limit and possibly discuss corrections to the master equation from higher order terms, as recently done.⁵⁵

C. Properties of the NCA propagator

The propagator $\mathcal{V}(t, t')$ obtained in NCA is the time-evolution superoperator of the reduced density operator of the impurity. Assuming to switch on the interaction with the baths at time $t = 0$, then the density operator of the impurity at time t is given by $\rho_I(t) = \mathcal{V}(t, 0) \rho_I(0)$. A time evolution superoperator must be a convex-linear, completely positive and trace-preserving map.⁴⁴ It is natural to ask which of these properties are preserved by the NCA approximation. \mathcal{V} is obviously a linear map, implying it is also convex linear. We proved that it is trace-preserving and that it preserves hermiticity (see the [supplementary material](#)), while proving or disproving whether the map is completely positive is a tough task⁵⁶ that will be addressed in the future. We stress that $\mathcal{V}(t, t')$ describes



FIG. 7. The NCA series of the self-energy Σ . The resummed series for Σ corresponds to its $k = 1$ diagrams, where the bare propagator \mathcal{V}_0 is replaced with the dressed one \mathcal{V} .

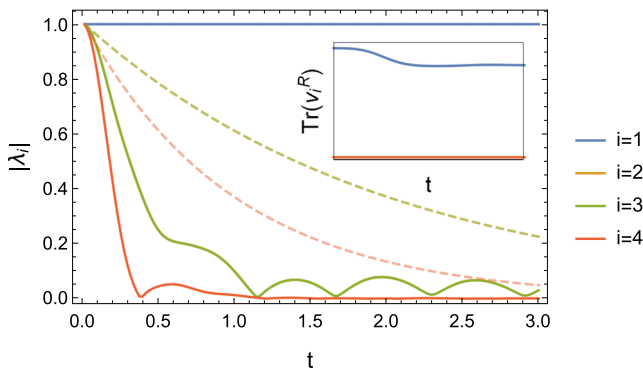


FIG. 8. Real-time evolution of the absolute value of the eigenvalues of the impurity propagator. While an eigenvector with eigenvalue one is present at all times, all the other eigenvalues decay to zero at long times. The $i = 2$ and $i = 3$ curves coincide because the corresponding eigenvalues are complex conjugates. The decay is purely exponential for a Markovian system, while strong deviations appear in the non-Markovian case. The inset shows that the right eigenstates of $\mathcal{V}(t)$ with different-from-one eigenvalues are traceless, while the right eigenstate with eigenvalue one has a finite (unnormalized) trace. Parameters: $\epsilon_0 = 5$, $\gamma = \gamma_l = \gamma_p = \gamma_d = 0.5$, $w = 10$, $\eta = 1$, $\Delta t = 0.02$, $\rho_0 = |0\rangle\langle 0|$.

a non-Markovian evolution, so it does not form a semigroup, that is, $\mathcal{V}(t, t') \neq \mathcal{V}(t, t_1)\mathcal{V}(t_1, t')$ with $t' < t_1 < t$. Time-evolution superoperators have also interesting spectral properties following from trace preservation. We refer to the [supplementary material](#) for the proof. We call $\lambda_i(t, t')$, $v_i^R(t, t')$ the eigenvalues and right eigenvectors of $\mathcal{V}(t, t')$, depending on time. As it preserves the trace, $\mathcal{V}(t, t')$ must have at least one eigenvalue equal to one, say $\lambda_0 \equiv 1$. If we assume this eigenvalue is nondegenerate, then all the other eigenvectors with $i \neq 0$ are traceless. As a consequence of these properties, if one evolves an initial state $\rho(0)$ and expands $\rho(t)$ on the instantaneous eigenvectors $v_i^R(t, 0)$, then those eigenvectors with $i \neq 0$ will represent decay modes of the dynamics as they will be suppressed by their corresponding vanishing eigenvalues for long times, while $v_{i=0}^R(t, 0)$ will evolve in time undumped until reaching a stationary value, representing the stationary state of the non-Markovian evolution. We will numerically check these properties in [Fig. 8](#) of [Sec. V](#), where we will apply our NCA algorithm to a specific example.

V. CASE STUDY: SPIN-LESS FERMIONIC IMPURITY

As a nontrivial application of the NCA approach for open systems described so far, we consider here a model of a single-mode, spin-less fermionic impurity with Markovian losses, pump, and dephasing and further coupled to a non-Markovian fermionic environment, as described in [Eq. \(1\)](#). We notice that the model in the absence of dephasing, also known as the resonant level model, is quadratic in all the fermionic degrees of freedom and therefore easily solvable, with analytical expressions known for the wide band limit. At finite dephasing, this is no longer the case and the model cannot, to the best of our knowledge, be solved by simple means. This could be understood naturally in the Keldysh approach, where the dephasing would result in density-density type of coupling between different Keldysh branches.

The Markovian dynamics is described by a Lindblad master equation,

$$\begin{aligned}\partial_t \rho_I^0 &= \mathcal{L} \rho_I^0, \\ \mathcal{L} \rho_I^0 &= -i[H_I, \rho_I^0] + (\gamma_l \mathcal{D}_l + \gamma_p \mathcal{D}_p + \gamma_d \mathcal{D}_d) \rho_I^0, \\ H_I &= \epsilon_0 d^\dagger d, \\ \mathcal{D}_l \rho_I^0 &= d \rho_I^0 d^\dagger - \frac{1}{2} \{d^\dagger d, \rho_I^0\}, \\ \mathcal{D}_p \rho_I^0 &= d^\dagger \rho_I^0 d - \frac{1}{2} \{dd^\dagger, \rho_I^0\}, \\ \mathcal{D}_d \rho_I^0 &= d^\dagger d \rho_I^0 d^\dagger d - \frac{1}{2} \{d^\dagger d, \rho_I^0\},\end{aligned}$$

where ϵ_0 is the energy of the fermionic level.

The effect of the non-Markovian environment on the impurity is completely determined by its hybridization function [\(10\)](#). Here, we choose a zero temperature, particle hole symmetric, fermionic bath with constant density of states of bandwidth $2w$ and with coupling strength to the impurity η . In this case, the hybridization function depends only on time-differences. As a consequence, one can show that also \mathcal{V} and Σ depend only on time differences and we will set $t' = 0$. With these definitions, we get for the hybridization functions

$$\begin{aligned}\Delta^{+-}(t) &= 2i\eta e^{iwt/2} \sin(wt/2)/t, \\ \Delta^{-+}(t) &= -2i\eta e^{-iwt/2} \sin(wt/2)/t.\end{aligned}$$

To solve the Dyson equation [\(25\)](#) numerically, we use the simple discretization scheme $\partial f(t) = [f(t + \Delta t) - f(t)]/\Delta t$, $\int_0^t dt_1 f(t_1) = \Delta t/2 \sum_{l=0}^{t/\Delta t-1} [f((l+1)\Delta t) + f(l\Delta t)]$, with time step Δt . More refined integration methods are explained in detail in [Ref. 45](#). The Hilbert space of the impurity has size $N = 2$ so that the superoperator \mathcal{V} has size $N^2 \times N^2 = 4 \times 4$.

A. Results

We start analyzing the spectral properties of the propagator $\mathcal{V}(t)$, which have been discussed generically in [Sec. IV C](#) and are reported in [Fig. 8](#). In the main panel, we plot the time dependence of the absolute value of the eigenvalues of $\mathcal{V}(t)$, both in the purely Markovian case (dashed lines) as well in the presence of both kind of dissipations. In both cases, there is an eigenvalue which remains equal to one, while the others decay to zero at long times, as pointed out in [Sec. IV C](#). However, the nature of this decay is rather different in the two cases, showing a faster dynamics and long time oscillations in the non-Markovian case as opposed to a pure exponential decay in the Markovian one. The inset of [Fig. 8](#) shows instead that all the right eigenstates of $\mathcal{V}(t)$ with different-from-one eigenvalues are traceless, while the right eigenstate with eigenvalue one has a finite trace (that we could normalize to one at every time).

We then consider the dynamics of a simple observable, such as the density of fermions in the impurity level, as a function of time and for different parameters (see [Fig. 9](#)). In the left figures, we plot the dynamics for different values of the coupling η (top) and bandwidth w (bottom) of the non-Markovian environment, in the presence of fixed Markovian losses, pump, and dephasing. We see that with respect to the purely Markovian dynamics, characterized by a simple exponential relaxation, the NCA approach captures aspects related to the non-Markovian nature of the environment.

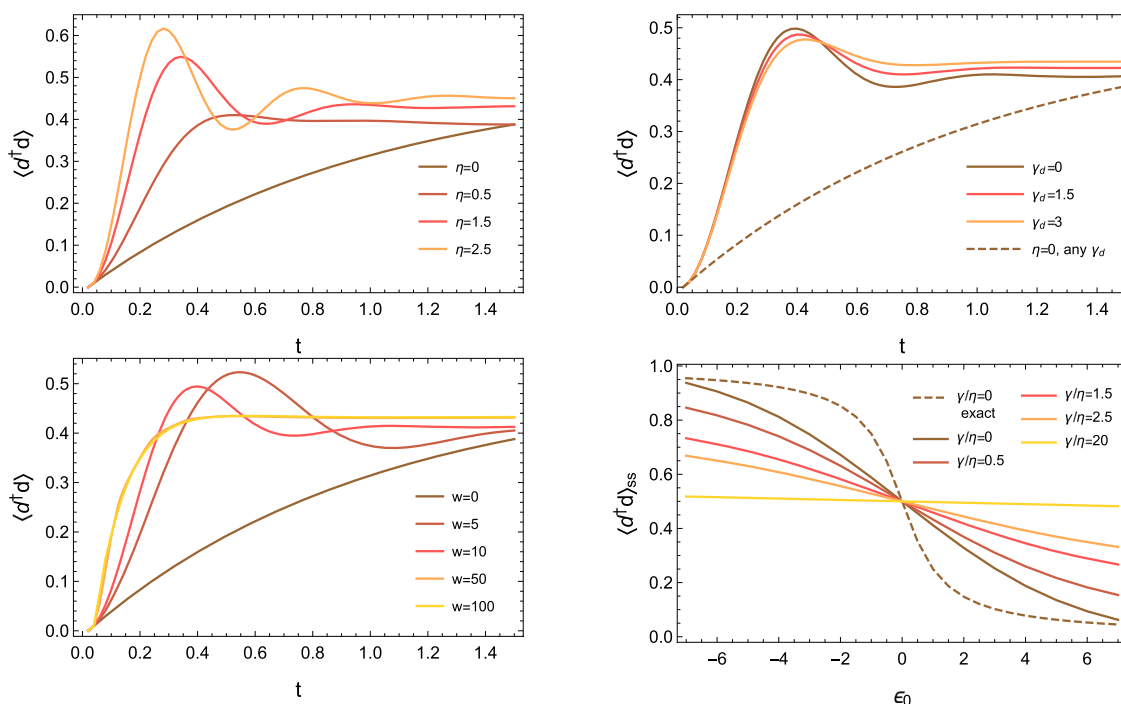


FIG. 9. Dynamics of the number of fermions for different sets of parameters, namely, changing the hybridization strength (top left), the bandwidth (bottom left), and the dephasing rate (top right). Average population of the stationary state as a function of the energy level (bottom right). Parameters: $\epsilon_0 = 1$, $\gamma = \gamma_l = \gamma_p = \gamma_d = 0.5$, $w = 10$, $\eta = 1$, $\Delta t = 0.02$, $\rho_0 = |0\rangle\langle 0|$.

In particular, the dynamics becomes characterized by oscillations whose amplitude and frequency increase with the coupling η . Similarly, increasing the bandwidth of the non-Markovian environment reduces the oscillations in the population dynamics, which disappear in the large bandwidth limit, as is the case for the unitary dynamics of the resonant level model. This is not surprising since oscillations at short-times $t \sim 1/w$ come from high-energy modes of the bath.

Overall, the non-Markovian environment makes the dynamics substantially faster. In the top-right plot, we discuss the role of dephasing, which is actually very interesting as it shows an effect of the combined Markovian and non-Markovian environments. The dashed line shows that, for Markovian dissipation only, the dephasing does not affect the population dynamics; this is well understood as the dephasing dissipator commutes with the number operator. It is interesting to see that, instead, combined with a non-Markovian environment the dephasing has an impact on the dynamics of populations; this is a smaller effect as it involves both the Markovian and the non-Markovian environments. This effect can be understood as follows: let us consider a process in the time-evolution in which the non-Markovian environment applies a d^\dagger_+ operator on the density matrix and then a d_+ operator after some time. The application of the creation operator converts the populations of the density matrix into coherences. Then, the Markovian dephasing dumps those coherences, which are then converted back to populations when the non-Markovian environment applies the annihilation operator. As a net effect, the dephasing has produced

a change into populations, as is shown in the top-right plot. We also note that not only the dynamics but also the stationary values of the occupation change with the dephasing. A more direct effect of the dephasing appears in the coherences, i.e., in the off-diagonal elements of the density matrix, which decay to zero faster as γ_d is increased, as we show in Fig. 10. For what concerns the stationary state, we notice from the bottom-right plot that the average density

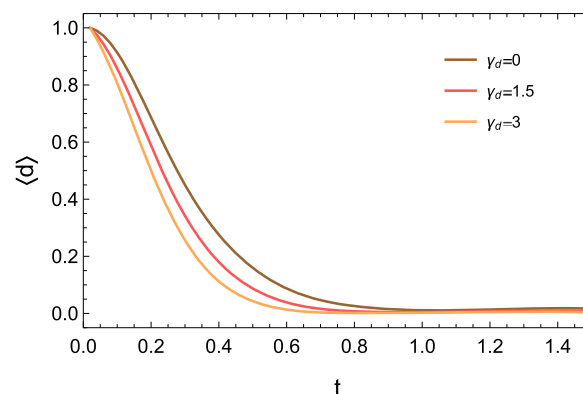


FIG. 10. Dynamics of the density matrix coherence for different values of the dephasing. Parameters: $\epsilon_0 = 1$, $\gamma = \gamma_l = \gamma_p = \gamma_d = 0.5$, $w = 10$, $\eta = 1$, $\Delta t = 0.02$, $\rho_0 = |0\rangle\langle 0| + |0\rangle\langle 1| + |1\rangle\langle 0|$.

would be independent of the energy of the fermionic level in the purely Markovian case, which leads to an infinite-temperature fully mixed stationary state for the chosen dissipation rates. This makes sense as a Markovian bath has no energy structure; thus, the level effectively sees always the same bath even if it is shifted in energy. On the other hand, the coupling to the non-Markovian bath makes the population depend strongly on the position of the energy level and gives a result which is in good agreement with exact analytical calculations (dashed line); to justify the quantitative discrepancy with this analytical result, we stress that for the noninteracting model we consider here that the NCA approximation, which is based on a strong coupling expansion, is not expected to be exact.

VI. CONCLUSIONS

In this work, we have focused on a model for a quantum impurity coupled simultaneously to a Markovian and a non-Markovian environment. We derived a formal hybridization expansion for the evolution superoperator of the impurity, obtained after tracing out all the bath degrees of freedom. This result generalizes the hybridization expansion, previously derived for quantum impurity models evolving under unitary dynamics, to the case of dissipative Markovian dynamics. As such, it provides the natural starting point for the development of stochastic sampling techniques of the dissipative real-time dynamics of the impurity based on diagrammatic Monte Carlo that we leave for future studies.

Starting from this expansion, we define real-time diagrammatic rules and write down a Dyson equation for the impurity propagator that we evaluate retaining only noncrossing diagrams, an approximation which is known to capture some aspects of the impurity physics at strong coupling. The resulting approach leads to a trace and hermiticity preserving the non-Markovian dynamical map, with consequences on the spectral properties of the evolution superoperator, while proving its complete positivity in full generality remains an open question.

It is interesting to comment on the relation between our approach and related methods to deal with impurity models coupled to multiple baths. While in principle both the hybridization expansion⁵⁷ and the strong coupling diagrammatic resummation⁵⁸ can be generalized in the presence of multiple environments, taking the Markovian limit from the start has some practical and conceptual advantage. In particular, we can take direct advantage of the local nature of the Markovian evolution and perform an expansion around an *atomic-limit* which now contains not only interaction but also drive and dissipation. This limit can be solved exactly by direct diagonalization of a Lindbladian, as opposed to treating exactly the degrees of freedom of the environment which are not expected to introduce new physics in the presence of memoryless Markovian correlations. The key idea is therefore to treat on equal footing all the energy scales related to fast processes, while resorting to perturbation theory when dealing with processes leading to slowing decay correlations such as the coupling to gapless reservoirs.

As an application, we solved numerically the Dyson equation for the simple model of a fermionic, single-mode impurity, with Markovian losses, pump, and dephasing and a non-Markovian,

zero temperature environment. This model is nontrivial for the presence of dephasing, which is a quartic term in fermionic operators. This simple implementation allowed to check the spectral properties of the evolution superoperator and to study how Markovian dynamics gets modified by coupling to a non-Markovian environment. In particular, our method allowed showing a physical consequence of coupling simultaneously to Markovian and non-Markovian environments: Markovian dephasing combined with non-Markovian processes leads to a change in impurity occupations. Future directions include the exploration of more complex impurity models involving internal degrees of freedom such as the Anderson impurity model as well as bosonic extensions and the use of this method as an impurity solver within a dynamical mean field theory approach to driven-dissipative systems.

SUPPLEMENTARY MATERIAL

The [supplementary material](#) includes (i) a derivation of the equation for the steady state density matrix starting from the Dyson equation for the non-Markovian map, (ii) the detailed derivation of the NCA self-energy, and (iii) the proofs of trace and hermiticity preservation of the NCA dynamics.

REFERENCES

- ¹A. O. Caldeira and A. J. Leggett, "Influence of dissipation on quantum tunneling in macroscopic systems," *Phys. Rev. Lett.* **46**, 211 (1981).
- ²A. J. Leggett, S. Chakravarty, A. T. Dorsey, M. P. A. Fisher, A. Garg, and W. Zwerger, "Dynamics of the dissipative two-state system," *Rev. Mod. Phys.* **59**, 1 (1987).
- ³K. L. Hur, L. Henriot, L. Herviou, K. Plekhanov, A. Petrescu, T. Goren, M. Schiro, C. Mora, and P. P. Orth, "Driven dissipative dynamics and topology of quantum impurity systems," *C. R. Phys.* **19**, 451–483 (2018).
- ⁴A. C. Hewson, *The Kondo Problem to Heavy Fermions* (Cambridge University Press, 1993).
- ⁵D. Goldhaber-Gordon *et al.*, "Kondo effect in a single-electron transistor," *Nature* **391**, 156 (1998).
- ⁶M. Grobis, I. G. Rau, R. M. Potok, H. Shtrikman, and D. Goldhaber-Gordon, "Universal scaling in nonequilibrium transport through a single channel Kondo dot," *Phys. Rev. Lett.* **100**, 246601 (2008).
- ⁷N. Roch, S. Florens, V. Bouchiat, W. Wernsdorfer, and F. Balestro, "Quantum phase transition in a single-molecule quantum dot," *Nature* **453**, 633 (2008).
- ⁸Z. Iftikhar, A. Anthore, A. K. Mitchell, F. D. Parmentier, U. Gennser, A. Ouerghi, A. Cavanna, C. Mora, P. Simon, and F. Pierre, "Tunable quantum criticality and super-ballistic transport in a 'charge' Kondo circuit," *Science* **360**, 1315–1320 (2018).
- ⁹G. Cohen and E. Rabani, "Memory effects in nonequilibrium quantum impurity models," *Phys. Rev. B* **84**, 075150 (2011).
- ¹⁰E. Gull, A. J. Millis, A. I. Lichtenstein, A. N. Rubtsov, M. Troyer, and P. Werner, "Continuous-time Monte Carlo methods for quantum impurity models," *Rev. Mod. Phys.* **83**, 349–404 (2011).
- ¹¹L. Mühlbacher and E. Rabani, "Real-time path integral approach to nonequilibrium many-body quantum systems," *Phys. Rev. Lett.* **100**, 176403 (2008).
- ¹²M. Schiró and M. Fabrizio, "Real-time diagrammatic Monte Carlo for nonequilibrium quantum transport," *Phys. Rev. B* **79**, 153302 (2009).
- ¹³P. Werner, T. Oka, and A. J. Millis, "Diagrammatic Monte Carlo simulation of nonequilibrium systems," *Phys. Rev. B* **79**, 035320 (2009).
- ¹⁴G. Cohen, E. Gull, D. R. Reichman, A. J. Millis, and E. Rabani, "Numerically exact long-time magnetization dynamics at the nonequilibrium Kondo crossover of the Anderson impurity model," *Phys. Rev. B* **87**, 195108 (2013).

- ¹⁵R. E. V. Profumo, C. Groth, L. Messio, O. Parcollet, and X. Waintal, "Quantum Monte Carlo for correlated out-of-equilibrium nanoelectronic devices," *Phys. Rev. B* **91**, 245154 (2015).
- ¹⁶G. Cohen, E. Gull, D. R. Reichman, and A. J. Millis, "Taming the dynamical sign problem in real-time evolution of quantum many-body problems," *Phys. Rev. Lett.* **115**, 266802 (2015).
- ¹⁷H.-T. Chen, G. Cohen, and D. R. Reichman, "Inchworm Monte Carlo for exact non-adiabatic dynamics. I. Theory and algorithms," *J. Chem. Phys.* **146**, 054105 (2017).
- ¹⁸H.-T. Chen, G. Cohen, and D. R. Reichman, "Inchworm Monte Carlo for exact non-adiabatic dynamics. II. Benchmarks and comparison with established methods," *J. Chem. Phys.* **146**, 054106 (2017).
- ¹⁹I. Bloch, J. Dalibard, and S. Nascimbène, "Quantum simulations with ultracold quantum gases," *Nat. Phys.* **8**, 267 (2012).
- ²⁰R. Blatt and C. F. Roos, "Quantum simulations with trapped ions," *Nat. Phys.* **8**, 277 (2012).
- ²¹A. A. Houck, H. E. Tureci, and J. Koch, "On-chip quantum simulation with superconducting circuits," *Nat. Phys.* **8**, 292 (2012).
- ²²K. L. Hur, L. Henriot, A. Petrescu, K. Plekhanov, G. Roux, and M. Schiró, "Many-body quantum electrodynamics networks: Non-equilibrium condensed matter physics with light," *C. R. Phys.* **17**, 808–835 (2016).
- ²³H.-P. Breuer and F. Petruccione, *The Theory of Open Quantum Systems*, 1st ed. (Oxford University Press, USA, 2002).
- ²⁴S. Diehl, A. Micheli, A. Kantian, B. Kraus, H. P. Buchler, and P. Zoller, "Quantum states and phases in driven open quantum systems with cold atoms," *Nat. Phys.* **4**, 878–883 (2008).
- ²⁵F. Verstraete, M. M. Wolf, and J. Ignacio Cirac, "Quantum computation and quantum-state engineering driven by dissipation," *Nat. Phys.* **5**, 633–636 (2009).
- ²⁶K. W. Murch, U. Vool, D. Zhou, S. J. Weber, S. M. Girvin, and I. Siddiqi, "Cavity-assisted quantum bath engineering," *Phys. Rev. Lett.* **109**, 183602 (2012).
- ²⁷M. Nakagawa, N. Kawakami, and M. Ueda, "Non-Hermitian Kondo effect in ultracold alkaline-earth atoms," *Phys. Rev. Lett.* **121**, 203001 (2018).
- ²⁸F. Tonielli, R. Fazio, S. Diehl, and J. Marino, "Orthogonality catastrophe in dissipative quantum many-body systems," *Phys. Rev. Lett.* **122**, 040604 (2019).
- ²⁹H. Fröml, A. Chiochetta, C. Kollath, and S. Diehl, "Fluctuation-induced quantum Zeno effect," *Phys. Rev. Lett.* **122**, 040402 (2019).
- ³⁰M. R. Delbecq, V. Schmitt, F. D. Parmentier, N. Roch, J. J. Vienne, G. Fève, B. Huard, C. Mora, A. Cottet, and T. Kontos, "Coupling a quantum dot, fermionic leads, and a microwave cavity on a chip," *Phys. Rev. Lett.* **107**, 256804 (2011).
- ³¹M. Schiró and K. Le Hur, "Tunable hybrid quantum electrodynamics from nonlinear electron transport," *Phys. Rev. B* **89**, 195127 (2014).
- ³²L. E. Bruhat, J. J. Vienne, M. C. Dartailh, M. M. Desjardins, T. Kontos, and A. Cottet, "Cavity photons as a probe for charge relaxation resistance and photon emission in a quantum dot coupled to normal and superconducting continua," *Phys. Rev. X* **6**, 021014 (2016).
- ³³A. Cottet, M. C. Dartailh, M. M. Desjardins, T. Cubaynes, L. C. Contamin, M. Delbecq, J. J. Vienne, L. E. Bruhat, B. Douçot, and T. Kontos, "Cavity QED with hybrid nanocircuits: From atomic-like physics to condensed matter phenomena," *J. Phys.: Condens. Matter* **29**, 433002 (2017).
- ³⁴B.-H. Liu, L. Li, Y.-F. Huang, C.-F. Li, G.-C. Guo, E.-M. Laine, H.-P. Breuer, and J. Piilo, "Experimental control of the transition from Markovian to non-Markovian dynamics of open quantum systems," *Nat. Phys.* **7**, 931–934 (2011).
- ³⁵Á. Rivas, S. F. Huelga, and M. B. Plenio, "Quantum non-Markovianity: Characterization, quantification and detection," *Rep. Prog. Phys.* **77**, 094001 (2014).
- ³⁶H.-P. Breuer, E.-M. Laine, J. Piilo, and B. Vacchini, "Colloquium: Non-Markovian dynamics in open quantum systems," *Rev. Mod. Phys.* **88**, 021002 (2016).
- ³⁷K. Haule, "Quantum Monte Carlo impurity solver for cluster dynamical mean-field theory and electronic structure calculations with adjustable cluster base," *Phys. Rev. B* **75**, 155113 (2007).
- ³⁸N. E. Bickers, "Review of techniques in the large-N expansion for dilute magnetic alloys," *Rev. Mod. Phys.* **59**, 845–939 (1987).
- ³⁹P. Nordlander, M. Pustilnik, Y. Meir, N. S. Wingreen, and D. C. Langreth, "How long does it take for the Kondo effect to develop?," *Phys. Rev. Lett.* **83**, 808–811 (1999); e-print [arXiv:9903240v1](https://arxiv.org/abs/9903240v1) [arXiv:cond-mat].
- ⁴⁰M. Eckstein and P. Werner, "Nonequilibrium dynamical mean-field calculations based on the noncrossing approximation and its generalizations," *Phys. Rev. B* **82**, 115115 (2010).
- ⁴¹A. Rüegg, E. Gull, G. A. Fiete, and A. J. Millis, "Sum rule violation in self-consistent hybridization expansions," *Phys. Rev. B* **87**, 075124 (2013).
- ⁴²H. U. R. Strand, M. Eckstein, and P. Werner, "Nonequilibrium dynamical mean-field theory for bosonic lattice models," *Phys. Rev. X* **5**, 011038 (2015).
- ⁴³F. Peronaci, M. Schiró, and O. Parcollet, "Resonant thermalization of periodically driven strongly correlated electrons," *Phys. Rev. Lett.* **120**, 197601 (2018).
- ⁴⁴H. Breuer and F. Petruccione, *The Theory of Open Quantum Systems* (OUP, Oxford, 2007).
- ⁴⁵H. Aoki, N. Tsuji, M. Eckstein, M. Kollar, T. Oka, and P. Werner, "Nonequilibrium dynamical mean-field theory and its applications," *Rev. Mod. Phys.* **86**, 779–837 (2014).
- ⁴⁶H. Carmichael, *Statistical Methods in Quantum Optics 1: Master Equations and Fokker-Planck Equations*, Physics and Astronomy Online Library (Springer, 1999).
- ⁴⁷J. Schwinger, "Brownian motion of a quantum oscillator," *J. Math. Phys.* **2**, 407–432 (1961).
- ⁴⁸L. V. Keldysh, "Diagram technique for nonequilibrium processes," *Zh. Eksp. Teor. Fiz.* **47**, 1515–1527 (1964).
- ⁴⁹P. Danielewicz, "Quantum theory of nonequilibrium processes II. Application to nuclear collisions," *Ann. Phys.* **152**, 305–326 (1984).
- ⁵⁰P. Danielewicz, "Quantum theory of nonequilibrium processes, I," *Ann. Phys.* **152**, 239–304 (1984).
- ⁵¹M. Wagner, "Expansions of nonequilibrium green's functions," *Phys. Rev. B* **44**, 6104–6117 (1991).
- ⁵²M. Schiró, "Real-time dynamics in quantum impurity models with diagrammatic Monte Carlo," *Phys. Rev. B* **81**, 085126 (2010).
- ⁵³C. W. Gardiner and M. J. Collett, "Input and output in damped quantum systems: Quantum stochastic differential equations and the master equation," *Phys. Rev. A* **31**, 3761–3774 (1985).
- ⁵⁴P. Werner, A. Comanac, L. de' Medici, M. Troyer, and A. J. Millis, "Continuous-time solver for quantum impurity models," *Phys. Rev. Lett.* **97**, 076405 (2006).
- ⁵⁵C. Müller and T. M. Stace, "Deriving Lindblad master equations with Keldysh diagrams: Correlated gain and loss in higher order perturbation theory," *Phys. Rev. A* **95**, 013847 (2017).
- ⁵⁶V. Reimer and M. R. Wegewijs, "Density-operator evolution: Complete positivity and the Keldysh real-time expansion," e-print [arXiv:1808.09395](https://arxiv.org/abs/1808.09395) (2018), 1–45.
- ⁵⁷D. Golež, M. Eckstein, and P. Werner, "Dynamics of screening in photodoped Mott insulators," *Phys. Rev. B* **92**, 195123 (2015).
- ⁵⁸H.-T. Chen, G. Cohen, A. J. Millis, and D. R. Reichman, "Anderson-Holstein model in two flavors of the noncrossing approximation," *Phys. Rev. B* **93**, 174309 (2016).